J Incl Phenom Macrocycl Chem (2009) 64:341–355
DOI 10.1007/s10847-009-9573-2

ORIGINAL ARTICLE

Theoretical and experimental study on metal(II) halide complexes of 1,3-bis(4-pyridyl)propane

Yusuf Erdogdu · M. Tahir Güllüoğlu · Mustafa Kurt · Şenay Yurdakul

Received: 9 July 2008 / Accepted: 13 March 2009 / Published online: 7 April 2009
© Springer Science+Business Media B.V. 2009

Abstract We report the results of detailed experimental and theoretical studies on the molecular structure and vibrational spectra of metal(II) halide complexes of 1,3-bis(4-pyridyl)propane [$M(N_2C_{13}H_{14})X_2$, where M represents Zn or Hg, and X represents Cl, Br, or I]. The FT–infrared spectra (FT-IR) and FT-Raman spectra of the metal complexes of the 1,3-bis(4-pyridyl)propane molecule in the powder form were recorded between the 400–4000 and 5–3500 cm^{-1} regions, respectively. The molecular geometry and vibrational frequencies of the metal complexes of 1,3-bis(4-pyridyl)propane in the ground state were calculated using density functional theory (B3LYP functional) with LANL2DZ and SDD as basis sets. The total energy distributions (TED) among the symmetry coordinates of the normal modes were computed for the low-energy structure of the molecules. Complete vibrational assignments based on the calculated TED values are given.

Keywords 1,3-bis(4-pyridyl)propane · Density functional theory · FT-IR spectra · FT-Raman Spectra · Metal(II) halide complexes

Electronic supplementary material The online version of this article (doi:10.1007/s10847-009-9573-2) contains supplementary material, which is available to authorized users.

Y. Erdogdu · M. T. Güllüoğlu (✉) · M. Kurt
Art and Science Faculty Department of Physics, Ahi Evran University, 40040 Kirsehir, Turkey
e-mail: mtahir@gazi.edu.tr

Ş. Yurdakul
Art and Science Faculty Department of Physics, Gazi University, 06500 Teknikokullar, Ankara, Turkey

Introduction

Supramolecular chemistry is the study of the chemistry and collective behavior of organized ensembles of molecules—of interactions between, rather than within, molecules. This field has attracted the attention of many research groups. The main challenges encountered in such studies are the strategic construction of specific supramolecular arrangements and comprehension of the relationship between these structures and their physical–chemical properties. 1,3-bis(4-pyridyl)propane (Bpp) is a very flexible versatile bifunctional ligand. The metal–organic coordination polymers of the Bpy [4,4′-pyridine] and Bpp ligands have attracted the continuous attention of researchers in recent years [1]. Two new coordination polymers with the general formula $[Mn(C_4O_4)(Bpp)_2(H_2O)]$ and $[Co(C_4O_4)(Bpp)_2(H_2O)$ where C_4O_4 = squarate ion] have been synthesized and characterized by vibrational spectroscopy [Raman and infrared (IR)], X-ray diffraction and termal analysis. These two compounds are isostructural, containing Bpp and the squarete ligand coordinated to the metal sites, as well as two water molecules, in a distorted octahedral geometry. The synthesis, crystal structure, and vibrational spectra of the coordination polymers with Bpp and squarate ion ligands and transition metal ions (M: Mn^{+2}, Co^{+2}, Ni^{+2}, Cu^{+2}, and Zn^{+2}) have been described [2, 3]. All compounds are isostructural, and Bpp is not coordinated to the metal site since it is in cationic form due to the protonation of N atoms from the pyridyl rings. An extensive literature on networks crystallized from different dipyridyl ligands with various transition metal ions now exists. Networks prepared from flexible dipyridyl ligands are of interest to many researchers because of the possible occurrence of different ligand conformations within the lattice. The presence of these different conformations means that

different topologies in polymeric structures can be attained using this ligand [4].

1,3-bis(4-pyridyl)propane is an interesting flexible bidentate ligand. The bpp molecule can adopt four discrete conformations [5–7]: *transoid–transoid* (*TT*), g*auche–gauche* (*GG*), *transoid–gauche* (*TG*), and *gauche–gauche′* (*GG′*) depending on the different N-to-N distances or dihedral angels. The Bpp ligand adopts the most stable *TT* conformation with dihedral angles of −180° (C_{20}–C_{17}–C_{14}–C_{11}) and 180° (C_{17}–C_{14}–C_{11}–C_3) [8, 9]. These N–N bond distances for these conformations have been determined to be in the range of 9.1–10.1 A° for the *TT* conformation, 8.6–9.2 A° for the *TG* conformation, 3.9–5.3 A° for the *GG* conformation, and 6.7–8.6 A° for *GG′* conformation [10, 11]. Based on these distances, free Bpp can be considered to be most stable in the *TT* conformation in the metal(II) halide complexes of Bpp.

In the study reported here, we investigated the molecular structure and vibrational spectra of the title complexes in their ground states. To the best of our knowledge, the experimental and theoretical spectroscopic properties of the title complexes have not yet been studied in detail. We compared the Fourier transform (FT)–IR and FT-Raman spectra of the title complexes with theoretical vibrational data and also compared the experimental vibrational spectra of the title complexes with those of free Bpp. In a recent investigation, we assignmed the vibrational modes of Bpp by means of quantum chemical calculations [8]. Here, the vibrational assignments of the normal modes were made based on the calculated total energy distribution (TED) values.

Computational details

Quantum chemical calculations were carried out with the Gaussian 03 program package [12], together with Gauss-view molecular visualization program [13]. The optimized geometry of the title complexes in the ground state were performed applying DFT (B3LYP) with the LANL2DZ and SDD basis sets. Vibrational spectra were calculated using this theory. The calculated harmonic frequencies were also scaled by corresponding scaling factor (http://srdata.nist.gov/cccbdb/vsf.asp). The TED of vibrational modes was calculated by using the scaled quantum mechanics (SQM) program [14].

Experimental

The Bpp molecule was purchased from the Sigma Aldrich Chemical Company (St. Louis, MO) with a stated purity >98%; it was used as such without further purification.

Table 1 Analytic data on the prepared complexes

Complexes	Carbon[a]	Nitrogen[a]	Hydrogen[a]
$Zn(BPP)Cl_2$	47.14/46.67	8.48/8.37	4.80/4.21
$Zn(BPP)Br_2$	37.11/37.13	6.66/6.72	3.32/3.35
$Zn(BPP)I_2$	30.17/29.78	5.41/5.11	2.72/2.70
$Hg(BPP)Cl_2$	33.52/33.23	6.03/5.96	3.53/3.00
$Hg(BPP)Br_2$	28.30/27.94	5.13/5.01	3.23/2.52
$Hg(BPP)I_2$	23.92/23.53	4.29/4.08	2.16/2.00

[a] Ratios represent the amount found/amount calculated and are expressed as a percentage

The $M(Bpp)X_2$; (M: Zn or Hg; X: Cl, Br, or I) complexes were prepared by the following method: metal salts (Cl, Br, or I) were dissolved in absolute ethanol (10 ml) to which 1 mmol of the Bpp solution in ethanol was then added. The mixture was stirred using a magnetic stirrer at room temperature. The precipitated complexes were filtered, washed with ether, and dried. The freshly prepared complexes were analyzed for C, H and N on a LECO-932 model analyzer (LECO Corp, St. Joseph, MI). The results of C, N and H analyses for the complexes are given in Table 1.

The title complexes are in powder forms at room temperature. The FT–IR spectra of the samples were recorded between 400 and 4000 cm^{-1} on a Mattson 1000 FT–IR spectrometer (Mattson, Freemont, CA) that was calibrated using polystyrene bands. The samples were prepared as a KBr disc. The FT-Raman spectra of the sample were recorded between the 5 and 3500 cm^{-1} region on a Bruker FRA 106/S FT-Raman instrument (Bruker, Billerica, MA) using 1064 nm excitation from an Nd:YAG laser. The detector is a liquid nitrogen-cooled Ge detector.

Results and discussion

Geometrical structures

The optimized bond lengths and bond angles of the title complexes are listed in Electronic Supplementary Material (ESM) Tables S1 and S2. The atom numbering scheme of the title complexes are shown in Fig. 1. Optimized geometric parameters of Zn title complexes and $Hg(Bpp)I_2$ are compared with corresponding published experimental data [15–17]. However, there is no published experimental data available on the $Hg(Bpp)Cl_2$ and $Hg(Bpp)Br_2$ complexes; consequently, we compared our data on these complexes with available data on other $Hg(Bpp)I_2$ complexes. The theoretical calculations pertain to isolated complexes in gaseous phase although the experimental results belong to complexes in solid phase. As seen in Tables S1 and S2, the experimental values are slightly larger than theoretical

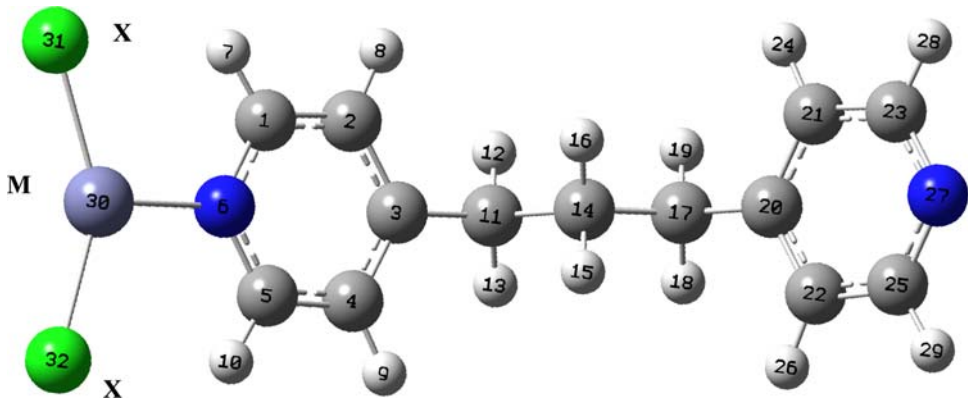

Fig. 1 Metal complexes of the 1,3-bis(4-pyridyl)propane (Bpp) structure and numbering of the atoms. *M*: Zn or Hg, *X*: Cl, Br, or I

values. In general, however, the calculated values are in good agreement with X-ray data of studied complexes.

The Bpp ligand molecule bridges the Zn(II) or Hg(II) atoms to form a one-dimensional chain complex. This structure; metal(II) atoms (M: Zn or Hg) is coordinated by two nitrogen atoms from the pyridine and two halide ligands. The coordinated geometric structure of the metal atom is a distorted tetrahedral, with the asymmetric unit of the title complexes containing half of the formula $M(Bpp)X_2$ (M: Zn or Hg; X: Cl, Br, or I). The whole chain is generated by two crystallographic mirror planes: one resides through X_{31}–M_{30}–X_{32}, and the other resides through H_{15}–C_{14}–H_{16}; these were obtained at 111.75° and 111.50° (N–Zn–N) for $Zn(Bpp)Cl_2$ and $Zn(Bpp)Br_2$, respectively [15, 16]. The calculated standard deviation of the difference (SDD) values of the corresponding angle was 107.20° and 105.77° for $Zn(Bpp)Cl_2$, $Zn(Bpp)Br_2$, respectively.

The Zn–X bond lengths of the title complexes were found to be slightly different: Zn–X bond lengths are predicted at 2.203 A° (for Cl), 2.336 A° (for Br), and 2.547 A° (I) in the calculations. As seen in Fig. 2a, both the LANL2DZ basis set and X-ray data increase in the same order I > Br > Cl. The Zn–X bond lengths of the Hg complexes are slightly larger than those of the Zn complexes.

The M–N bond lengths are between 2.045 A° and 2.509 A°. As seen Fig. 2b, the order of the M–N bond lengths are $Zn(Bpp)Cl_2$ (2.081 A°) < $Zn(Bpp)Br_2$ (2.090 A°) < $Zn(Bpp)I_2$ (2.102 A°) and $Hg(Bpp)Cl_2$ (2.481 A°) < $Hg(Bpp)Br_2$ (2.479 A°) < $Hg(Bpp)I_2$ (2.509 A°) for the LANL2DZ basis set. The order of the M–N bond lengths are $Hg(Bpp)Cl_2$ (2.454 A°) > $Zn(Bpp)Cl_2$ (2.045 A°) and $Hg(Bpp)Br_2$ (2.460 A°) > $Zn(Bpp)Br_2$ (2.048 A°) for the SDD basis set. The M–N bond lengths of Zn complexes are about 0.3 A° (SDD) and 0.45 A° (LANL2DZ) shorter than those of the Hg complexes. It is noted that the M–N bond length values depend on the halogen for a given metal complex and that they decrease in the order I > Br > Cl [18].

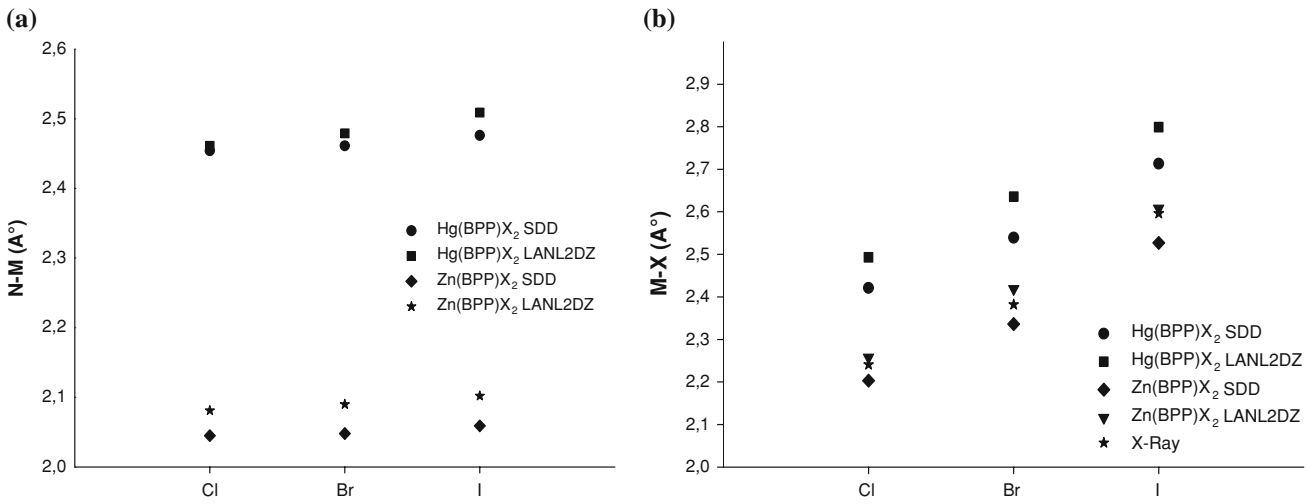

Fig. 2 The N–M (**a**) and M–X (**b**) bond lengths of the metal complexes of Bpp. *M*: Zn or Hg, *X*: Cl, Br, or I

Vibrational assignments

The metal complexes of Bpp consist of 32 atoms with C_S symmetry. The 90 normal vibrations are distributed as 49 A′ (in-plane) + 41 A″ (out-of-plane). All of the vibrations are active in both FT-IR and FT-Raman spectra. The calculated frequencies with experimental data of the ligand are presented in Tables 2 and 3. Theoretically computed IR and Raman spectra of M(Bpp)X2 (M: Zn or Hg; X: Cl, Br, or I) are given in Figs. S1 and S2 of the ESM. The FT-IR and FT-Raman spectra of the title complexes are illustrated in Figs. 3 and 4.

Analysis of the hetero-aromatic structure shows the presence of C–H stretching vibrations in the region 3000–3200 cm^{-1}, which is the characteristic region for the ready identification of C–H stretching vibrations. In this study, the C–H stretching vibrations of the pyridine rings were observed at 3057 (Cl), 3055 (Br) and 3057 cm^{-1} (I) in the FT–IR spectra of the Zn complexes; this peak was observed at 3051 cm^{-1} for the free ligand in the FT-IR spectra [8]. The other C–H peak was observed at 3040 (Cl), 3037 (Br), 3034 cm^{-1} (I) in the FT-IR spectra of the Zn complexes; the corresponding peak was observed at 3029 cm^{-1} for the free ligand [8]. We observed that these vibrations shifted slightly to higher frequencies in the FT-IR and FT-Raman spectra of the title complexes.

The C–H stretching of the methylene groups are at lower frequencies than those of the aromatic ring. The CH_2 stretching vibrations of the free Bpp molecule were observed at 2905, 2929, 2944 and 2971 cm^{-1} in the FT–IR spectra and at 2902, 2927 and 2975 cm^{-1} in the FT-Raman spectra [8]. The CH_2 stretching vibrations of the Zn metal complexes were observed at 2933, 2954, 2989 cm^{-1} (Cl) in the FT-IR spectra of the Zn complexes. The CH_2 stretching vibrations of Hg complexes were observed at 2930, 2952, and 2983 cm^{-1} (Cl) in the FT-IR spectra of the Hg complexes. Out-of-plane rocking CH_2 mode of the free ligand appeared at 831 (IR) and 826 cm^{-1} (Ra) [8]. This peak was observed at 837 [for $Hg(Bpp)Cl_2$] and 838 cm^{-1} [for $(Zn(Bpp)Cl_2$] in the FT–IR spectra. The theoretically computed value shows an excellent agreement with experimental results.

Asymmetric CH_2 stretching vibrations were seen to shift slightly towards higher frequencies, whereas symmetric CH_2 stretching was observed to shift slightly towards lower frequencies in the FT–IR and FT–Raman spectra of metal complexes. The symmetric CH_2 and asymmetric CH_2 stretching vibrations of the Zn and Hg complexes are shown in Figs. 5 and 6, respectively.

The spectral region between 1600 and 1650 cm^{-1}, where ring stretching modes are expected, is very important in the Bpp ligand coordination analysis. The ring stretching band shows up at 1605 cm^{-1} for the free ligand; this peak has been observed to shift to higher frequencies (around 1620 cm^{-1}) when Bpp is coordinated to the metal ion [1, 5]. In the free ligand molecule, this band was observed at 1605 and 1606 cm^{-1} in the FT-IR and FT-Raman spectra, respectively [8]. In our study, the peak ring stretching vibrations of the Hg complexes were observed at 1611 (Cl), 1610 (Br), and 1608 cm^{-1} (I) in the FT-IR spectra; in comparison, these peaks were observed at 1619 (Cl), 1619 (Br), and 1618 cm^{-1} (I) in the FT-IR spectra of the Zn complexes. The ring stretching vibrations of the Zn complexes are slightly larger than those of the Hg complexes (Fig. 7).

The bands between 220 and 300 cm^{-1} are assigned to M–N stretching vibration. We expect that the υ(M–N) mode will shift to lower frequencies with increasing M–N bond lengths. The υ(M–N) mode of the Zn complexes is larger than that of the Hg complexes and, therefore, the M–N bond lengths in the Hg complexes are larger than those of the Zn complexes. This mode was observed experimentally at 249 (for Cl_2), 240 (for Br_2), and 232 cm^{-1} (for I_2) in the FT-Raman spectra of the Hg complexes. This peak was observed at 238 (for Cl_2), 224 (for Br_2) and 222 cm^{-1} (for I_2) in the FT-Raman spectra of the Zn complexes. As seen in Fig. 2a and Tables S1 and S2, in the complexes studied, decreases in the calculated M–N bond lengths in the order I > Br > Cl occurred concurrently with increases in the M–N stretching frequencies.

The total shifts are given at the bottom of Tables 2 and 3. For any given metal, therefore, it should be possible to compare the shift values of the isomorphous complexes as well as observe the effect of changing the stoichiometry of the complex and of changing the counter ligand from Cl, Br, and I. These shift values for isomorphous complexes show a progressive increase across the period from Zn to Hg, and this correlates with increases in the second ionization potential of metals [20, 21]. Similar shifts were observed in the vibrational spectra of pyridine and pyridine derivative halide complexes [19–21] and were explained by the mechanical coupling of pyridine (or pyridine derivative) vibrations with the M–N (pyridine or pyridine derivative) vibrational modes [19, 21, 22]. Therefore, we infer that the M–N (Bpp) bond strength and thus the M–N [1,3-bis(4-pyridyl)propane] stretching mode frequency increase in the same order. It is also noted that for isomorphous complexes the shift values depend on the halogen and that for a given metal, it decreases in the order Cl > Br > I.

Conclusion

The molecular structure and vibrational frequencies of the title complexes have been calculated using the

Table 2 Comparison of the observed and calculated vibrational spectra of Zn (Bpp)X_2 (X: Cl, Br, I) complexes

No	Symm. Spec	$Zn(Bpp)Cl_2$				$Zn(Bpp)Br_2$			
		LANL2DZ Freq.[a]	SDD[b] Freq.[b]	Exp. IR	Exp. RA	LANL2DZ[a] Freq.[a]	SDD[b] Freq.[b]	Exp. IR	Exp. RA
ν_1	A″	5	8			4	4		
ν_2	A″	16	16			13	14		
ν_3	A′	21	21			17	17		
ν_4	A″	42	41			36	35		
ν_5	A″	47	45			38	38		
ν_6	A′	54	57			49	51		
ν_7	A″	67	67			60	60		
ν_8	A″	85	84			66	68		
ν_9	A′	89	93			87	88		
ν_{10}	A′	92	102			89	93		
ν_{11}	A′	137	140		112 vs	131	133		103 vs
ν_{12}	A″	166	169			157	160		
ν_{13}	A′	172	170		153 vw	157	162		157 vw
ν_{14}	A′	244	244		218 vw	196	208		195 vw
ν_{15}	A′	253	251		249 w	244	245		240 w
ν_{16}	A′	289	306		284 s	254	253		276 m
ν_{17}	A″	327	327			285	301		
ν_{18}	A′	338	338			328	327		
ν_{19}	A″	340	340			338	338		
ν_{20}	A″	371	378		350 w	342	342		353 w
ν_{21}	A″	378	393			378	377		
ν_{22}	A″	396	397	407 vw		394	395	410 vw	
ν_{23}	A′	505	505			505	505		
ν_{24}	A′	520	519	519 s	522 vw	519	519	517 s	
ν_{25}	A′	583	583	593 vw		583	583	590 vw	
ν_{26}	A′	605	604	621 s	618 vw	604	604	620 s	
ν_{27}	A″	656	656			656	657		
ν_{28}	A″	658	658	671 w	666 w	658	658	671 w	666 m
ν_{29}	A′	741	740			741	740		
ν_{30}	A″	741	740	733 vw		742	741	732 w	
ν_{31}	A′	748	747	744 vw	744 w	748	747	744 vw	
ν_{32}	A′	782	781			782	782		
ν_{33}	A′	813	813	810 w		814	813	809 w	
ν_{34}	A′	835	835	824 s	825 m	835	835	822 s	824 w
ν_{35}	A″	836	836	838 vw		837	836	839 vw	
ν_{36}	A′	853	854	859 vw	861 m	852	854	857 m	857 m
ν_{37}	A″	883	883	878 w		883	883	876 w	
ν_{38}	A″	889	891			888	889		
ν_{39}	A′	953	953			953	953		
ν_{40}	A′	964	963	970 vw	965 vw	964	964	969 vw	
ν_{41}	A″	980	980			980	980		
ν_{42}	A′	988	988	988 vw	987 vw	987	989	989 vw	
ν_{43}	A′	1000	1000			999	999		
ν_{44}	A′	1002	1002			1000	1001		
ν_{45}	A″	1002	1005			1001	1005		
ν_{46}	A′	1010	1009			1009	1009		

Table 2 continued

No	Symm. Spec	$Zn(Bpp)Cl_2$				$Zn(Bpp)Br_2$			
		LANL2DZ Freq.[a]	SDD[b] Freq.[b]	Exp. IR	Exp. RA	LANL2DZ[a] Freq.[a]	SDD[b] Freq.[b]	Exp. IR	Exp. RA
ν_{47}	A″	1014	1013		1025 vw	1014	1014		1023 w
ν_{48}	A′	1046	1046	1031 s	1035 s	1046	1046	1030 s	1032 s
ν_{49}	A′	1049	1049			1049	1049		
ν_{50}	A″	1061	1060	1074 s	1071 w	1062	1061	1072 s	
ν_{51}	A″	1094	1093			1094	1094		
ν_{52}	A″	1118	1118	1112 vw		1119	1119	1110 vw	
ν_{53}	A′	1201	1201			1202	1201		
ν_{54}	A′	1205	1204			1205	1204		
ν_{55}	A′	1207	1207			1208	1208		
ν_{56}	A′	1216	1215			1219	1217		
ν_{57}	A″	1230	1229	1221 m	1218 s	1231	1230	1223 m	1216 s
ν_{58}	A′	1241	1241			1243	1242		
ν_{59}	A″	1260	1260	1263 vw	1258 vw	1261	1260	1260 vw	1256 vw
ν_{60}	A″	1273	1273			1274	1273		
ν_{61}	A″	1282	1277		1276 vw	1282	1277		
ν_{62}	A′	1309	1308	1305 vw	1303 vw	1310	1310	1305 vw	
ν_{63}	A″	1327	1327	1323 w	1322 m	1328	1327	1320 w	1320 m
ν_{64}	A′	1332	1331	1359 w	1345 vw	1332	1332	1358 w	
ν_{65}	A″	1332	1332	1377 vw		1334	1334	1375 vw	
ν_{66}	A″	1388	1387	1400 w		1388	1387	1394 w	
ν_{67}	A″	1410	1410	1432 s	1432 m	1411	1410	1432 s	1430 m
ν_{68}	A′	1454	1453	1447 vw		1454	1453	1447 vw	
ν_{69}	A′	1459	1458	1456 w		1459	1458	1457 w	
ν_{70}	A′	1466	1465			1467	1466		
ν_{71}	A′	1473	1472	1474 vw		1474	1473		
ν_{72}	A′	1479	1478	1488 vw		1479	1478		
ν_{73}	A″	1532	1530	1508 m	1507 vw	1532	1529	1509 m	1509 w
ν_{74}	A″	1540	1540	1542 vw		1540	1540	1541 vw	
ν_{75}	A′	1569	1568	1562 m	1557 vw	1569	1568	1562 m	
ν_{76}	A′	1594	1593	1619 vs	1621 s	1595	1594	1619 vs	1620 m
ν_{77}	A′	2926	2926			2926	2926		
ν_{78}	A′	2931	2930	2933 w	2930 s	2931	2930	2933 w	2920 s
ν_{79}	A′	2939	2938	2954 vs		2940	2938	2951 vs	2949 m
ν_{80}	A″	2967	2966			2967	2966		
ν_{81}	A″	2982	2980	2989 w	2955 w	2982	2981	2984 w	–
ν_{82}	A″	3004	3003			3005	3004		
ν_{83}	A″	3071	3071	3040 s	3038 w	3071	3072	3037 s	3036 m
ν_{84}	A′	3072	3072	3057 m	3067 vs	3072	3072	3055 m	3063 vs
ν_{85}	A″	3092	3092			3092	3093		
ν_{86}	A″	3094	3094			3094	3095		
ν_{87}	A′	3096	3096			3095	3096		
ν_{88}	A′	3099	3099			3099	3099		
ν_{89}	A″	3112	3112			3111	3112		
ν_{90}	A′	3117	3117			3116	3118		
				218				198	

Table 2 continued

No	Symm. Spec	$Zn(Bpp)I_2$				Free Bpp [8]		
		LANL2DZ[a] Freq.[a]	SDD[b] Freq.[b]	Exp. IR	Exp. RA	Exp. IR	Exp. RA	TED (%)
ν_1	A″	3	3					$\Gamma_{HCCC}(89)(M)$
ν_2	A″	12	12					$\Gamma_{HCCC}(33)$ (M) + $\Gamma_{HCCC}(51)$(P-M)
ν_3	A′	15	16					$\delta_{CCC}(27)(M) + \Gamma_{CCCC}$ (15) + $\Gamma_{MNCC}(12)$
ν_4	A″	32	32					$\delta_{XMN}(11) + \Gamma_{HCCC}(30)(M) + \Gamma_{CCCC}(27)(M)$
ν_5	A″	35	36					$\Gamma_{XMNC}(93)$
ν_6	A′	45	48					$\delta_{CCC}(19)(M) + \Gamma_{MNCC}(19) + \Gamma_{MNCH}(10) + \Gamma_{XMNC}(23)$
ν_7	A″	54	57					$\delta_{MNC}(14) + \delta_{XMN}(62)$
ν_8	A″	57	58					$\Gamma_{HCCC}(70) + \Gamma_{CCCC}(30)(M)$
ν_9	A′	83	88					$\delta_{XMX}(60) + \delta_{XMN}(30)$
ν_{10}	A′	91	90					$\Gamma_{CCCC}(14)$(P-M) + $\Gamma_{XMNC}(56)$
ν_{11}	A′	115	120		95 vs		91 vs	$\upsilon_{MN}(12) + \delta_{CCC}(10)(M) + \Gamma_{XMNC}(19)$
ν_{12}	A″	141	147					$\upsilon_{MN}(36) + \delta_{CCC}(10)(M)$
ν_{13}	A′	149	157		155 vw		155 vw	δ_{MNC} (61) + $\delta_{XMN}(26)$
ν_{14}	A′	180	184		186 vw		221 w	$\upsilon_{CC}(12) + \upsilon_{MN}(13) + \Gamma_{CCCC}(20)$(P-M)
ν_{15}	A′	243	243		232 w			$\upsilon_{MN}(20)$
ν_{16}	A′	244	251		274 m			$\upsilon_{MX}(99)$
ν_{17}	A″	252	257					$\delta_{CCC}(77)$(P-M)
ν_{18}	A′	328	327					$\delta_{CCC}(25)(M) + \Gamma_{CCCC}(18)$
ν_{19}	A″	338	338					$\delta_{CCC}(70)(M) + \delta_{MNC}(7)$
ν_{20}	A″	342	342		350 w		346 w	$\Gamma_{CCCC}(18) + \Gamma_{NCCC}(41) + \Gamma_{CNCC}(10) + \Gamma_{NCCH}(14)$
ν_{21}	A″	377	377					$\upsilon_{MX}(99)$
ν_{22}	A″	393	394	406 vw		403 vw	410 vw	$\Gamma_{CCCC}(17) + \Gamma_{NCCC}(36) + \Gamma_{NCCH}(12) + \Gamma_{CCCH}(13)$
ν_{23}	A′	504	504					$\upsilon_{C\text{-}CH2}(11) + \delta_{CCC}(11) + \delta_{CNC}(7)$
ν_{24}	A′	518	518	518 s		505 s	506 w	Γ_{CNCC} (11) + Γ_{CNCH} (10)
ν_{25}	A′	583	583	590 vw				$\delta_{CCC}(16)(M)$
ν_{26}	A′	603	603	618 s		603 s		$\delta_{CCC}(12)$(P-M) + $\delta_{CCC}(19) + \delta_{CNC}(10)$
ν_{27}	A″	656	657					$\delta_{CCC}(17) + \delta_{NCC}(30) + \delta_{CCH}(17)$
ν_{28}	A″	658	658	668 w	666 m	670 vw	668 m	$\delta_{CCC}(17) + \delta_{NCC}(32) + \delta_{CCH}(17)$
ν_{29}	A′	740	740					$\Gamma_{HCCH}(62)(M)$
ν_{30}	A″	743	741	730 w				$\Gamma_{CCCC}(14) + \Gamma_{NCCC}(18) + \Gamma_{CNCC}(21)$
ν_{31}	A′	748	747	741 vw		743 w	745 vw	$\Gamma_{NCCC}(18) + \Gamma_{CNCC}(13)$
ν_{32}	A′	782	782					$\upsilon_{CC}(25) + \upsilon_{C\text{-}CH2}(26) + \delta_{CNC}(14)$
ν_{33}	A′	814	814	809 w		784 s	799 vw	$\upsilon_{CC}(10) + \Gamma_{CCCH}(19) + \Gamma_{NCCH}(10)$
ν_{34}	A′	836	835	820 s				$\upsilon_{CC}(15) + \upsilon_{CC}(22)(M) + \Gamma_{CCCH}$ (23)
ν_{35}	A″	837	836	836 vw		831 s	826 w	$\delta_{CCH}(17) + \Gamma_{CCCH}(25)(M)$
ν_{36}	A′	851	853	856 m		855 s	863 m	$\Gamma_{CCCH}(23) + \Gamma_{NCCH}(15) + \Gamma_{CCCH}(19)$(P-M)
ν_{37}	A″	883	884					$\Gamma_{CCCH}(61) + \Gamma_{NCCH}(22) + \Gamma_{CNCH}(16)$
ν_{38}	A″	886	888					Γ_{CCCH} (34) + $\Gamma_{NCCH}(21) + \Gamma_{CCCH}(22)$(P-M) + $\Gamma_{CNCH}(11)$
ν_{39}	A′	953	953					$\upsilon_{CC}(22) + \upsilon_{CN}(38) + \delta_{CCH}(14)$
ν_{40}	A′	964	964	967 w				$\Gamma_{HCCH}(48) + \Gamma_{CC}7)$
ν_{41}	A″	980	980					$\Gamma_{CNCH}(18) + \Gamma_{HCCH}(48) + \Gamma_{CCCH}(22)$
ν_{42}	A′	985	988	984 vw		991 s	994 s	$\upsilon_{CC}(15) + \Gamma_{HCCH}(33) + \Gamma_{CCCH}(10)$
ν_{43}	A′	996	996					$\upsilon_{CC}(42)(M) + \upsilon_{CN}(14)$
ν_{44}	A′	998	1001					$\upsilon_{CC}(28) + \upsilon_{CN}(10)$
ν_{45}	A″	1000	1004					$\Gamma_{HCCH}(42) + \Gamma_{CNCH}(14) + \Gamma_{MNCH}(14)$

Table 2 continued

No	Symm. Spec	$Zn(Bpp)I_2$				Free Bpp [8]		
		LANL2DZ[a] Freq.[a]	SDD[b] Freq.[b]	Exp. IR	Exp. RA	Exp. IR	Exp. RA	TED (%)
ν_{46}	A′	1009	1009					$\upsilon_{CC}(58) + \delta_{HCC}(10)$(M)
ν_{47}	A″	1015	1014					$\upsilon_{CC}(14) + \delta_{HCC}(19)$(M) + $\Gamma_{HCCC}(33)$(Py-M)
ν_{48}	A′	1045	1046	1028 s	1019 s	1021 w	1021 w	$\upsilon_{CC}(11) + \upsilon_{CN}(29) + \delta_{CCC}(11) + \delta_{NCC}(12) + \delta_{CCH}(24)$
ν_{49}	A′	1049	1049					$\upsilon_{CC}(12) + \upsilon_{CN}(20) + \delta_{CCC}(12) + \delta_{NCC}(14) + \delta_{CCH}(27)$
ν_{50}	A″	1063	1062	1069 s		1065 w	1077 w	$\upsilon_{CC}(21) + \delta_{CCH}(15)$(M)
ν_{51}	A″	1095	1094					$\upsilon_{CC}(31) + \delta_{CCH}(28)$(M)
ν_{52}	A″	1120	1120	1111 vw	1130 w	1092 w		$\upsilon_{CC}(10) + \delta_{CCH}(21)$(M)
ν_{53}	A′	1202	1202					$\upsilon_{CC}(10) + \upsilon_{C\text{-}CH2}(31) + \delta_{CCH}(24)$
ν_{54}	A′	1205	1205					$\upsilon_{CC}(16) + \upsilon_{CN}(14) + \delta_{CCH}(29) + \delta_{NCH}(23)$
ν_{55}	A′	1208	1208					$\upsilon_{CC}(15) + \upsilon_{C\text{-}CH2}(28) + \delta_{CCH}(24)$
ν_{56}	A′	1220	1218					$\upsilon_{CC}(24) + \upsilon_{CN}(10) + \delta_{CCH}(18) + \delta_{NCH}(23)$
ν_{57}	A″	1231	1230	1224 m	1214 m	1227 m		$\delta_{CCH}(27)$(M)
ν_{58}	A′	1244	1243					$\delta_{CCH}(47) + \Gamma_{HCCH}(15)$(M)
ν_{59}	A″	1261	1260	1259 vw	1264 w	1252 vw	1253 w	$\upsilon_{CC}(54) + \upsilon_{CN}(32) + \delta_{CCH}(10)$(M)
ν_{60}	A″	1274	1274					$\upsilon_{CC}(7) + \upsilon_{CN}(13) + \delta_{CCH}(46)$(M)
ν_{61}	A″	1281	1277					$\upsilon_{CC}(26) + \upsilon_{CN}(44) + \delta_{CCH}(15)$(M)
ν_{62}	A′	1311	1311	1308 vw		1300 vw		$\delta_{CCH}(47) + \Gamma_{HCCC}(15)$(M)
ν_{63}	A″	1328	1327	1320 w	1318 w	1318 vw	1318 vw	$\delta_{CCH}(59) + \delta_{NCH}(18)$
ν_{64}	A′	1333	1332	1361 w		1340 m	1341 m	$\delta_{CCH}(42) + \Gamma_{HCCH}(19)$(M)
ν_{65}	A″	1335	1335			1361 vw		$\delta_{CCH}(60) + \delta_{NCH}(18)$
ν_{66}	A″	1388	1387	1391 w		1376 vw		$\upsilon_{CC}(24) + \delta_{CCH}(25) + \delta_{NCH}(30)$
ν_{67}	A″	1410	1410	1431 s		1416 s	1411 m	$\upsilon_{CC}(32) + \delta_{CCH}(23) + \delta_{NCH}(30)$
ν_{68}	A′	1454	1453			1441 w	1440 m	$\upsilon_{CN}(12) + \delta_{CCH}(34) + \delta_{NCH}(20)$
ν_{69}	A′	1459	1458	1456 w		1456 m		$\delta_{HCH}(26) + \Gamma_{HCCH}(38)$
ν_{70}	A′	1467	1466					$\delta_{HCH}(30) + \Gamma_{HCCH}(29)$
ν_{71}	A′	1474	1474	1475 vw		1475 vw		$\upsilon_{CC}(13) + \delta_{CCH}(48) + \delta_{NCH}(19)$
ν_{72}	A′	1479	1478					$\delta_{HCH}(30) + \Gamma_{HCCH}(29)$(M)
ν_{73}	A″	1532	1529	1507 m	1505 m	1501 m	1509 vw	$\upsilon_{CC}(49) + \upsilon_{CN}(25)$
ν_{74}	A″	1540	1540	1541 vw		1542 vw		$\upsilon_{CC}(48) + \upsilon_{CN}(27)$
ν_{75}	A′	1569	1568	1558 m		1557 m	1557 w	$\upsilon_{CC}(78) + \delta_{CCH}(15)$
ν_{76}	A′	1594	1593	1618 vs	1620 s	1605 vs	1606 m	$\upsilon_{CC}(79) + \delta_{NCH}(8) + \delta_{CCH}(9)$
ν_{77}	A′	2926	2926					$\upsilon_{CH2}(99)$
ν_{78}	A′	2931	2930	2930 w	2922 m	2929 w	2927 w	$\upsilon_{CH2}(100)$
ν_{79}	A′	2940	2939	2948 vs	2949 s	2944 vs		$\upsilon_{CH2}(100)$
ν_{80}	A″	2967	2966					$\upsilon_{CH2}(100)$
ν_{81}	A″	2982	2981	–	–	2971 vw	2975 vw	$\upsilon_{CH2}(97)$
ν_{82}	A″	3005	3004					$\upsilon_{CH2}(100)$
ν_{83}	A″	3071	3072	3034 s	3034 s	3029 m	3031 w	$\upsilon_{CH}(100)$
ν_{84}	A′	3072	3072	3057 m	3059 vs	3051 w	3056 vs	$\upsilon_{CH}(100)$
ν_{85}	A″	3092	3093					$\upsilon_{CH}(99)$
ν_{86}	A″	3092	3093					$\upsilon_{CH}(100)$
ν_{87}	A′	3094	3095					$\upsilon_{CH}(100)$
ν_{88}	A′	3099	3099					$\upsilon_{CH}(99)$
ν_{89}	A″	3109	3110					$\upsilon_{CH}(99)$
ν_{90}	A′	3114	3115					$\upsilon_{CH}(99)$
				166				Total Shifts

Table 3 Comparison of the observed and calculated vibrational spectra of Hg (Bpp)X_2 (X: Cl, Br or I) complexes

No	Symm. Spec	Hg (Bpp)Cl_2				Hg (Bpp)Br_2			
		LANL2DZ[a] Freq.[a]	SDD[b] Freq.[b]	Exp. IR	Exp. RA	LANL2DZ[a] Freq.[a]	SDD[b] Freq.[b]	Exp. IR	Exp. RA
ν_1	A″	10	9			3	3		
ν_2	A″	13	14			12	13		
ν_3	A′	16	17			15	18		
ν_4	A″	36	33			27	31		
ν_5	A″	45	37			36	34		
ν_6	A′	50	52			39	45		
ν_7	A″	53	54			48	51		
ν_8	A″	69	76			50	54		
ν_9	A′	69	77			62	67		
ν_{10}	A′	89	87			90	88		
ν_{11}	A′	98	92		89 vs	95	90		
ν_{12}	A″	127	127		110 vs	123	123		105 vs
ν_{13}	A′	130	131		157 vw	130	131		168 vw
ν_{14}	A′	226	224		207 vw	161	173		211 vw
ν_{15}	A′	241	241		238 w	211	224		224 w
ν_{16}	A′	262	276			225	231		
ν_{17}	A″	305	327		278 s	241	241		253 s
ν_{18}	A′	327	330			327	327		
ν_{19}	A″	334	333			333	333		
ν_{20}	A″	337	336		353 w	336	336		352 w
ν_{21}	A″	378	378			378	378		
ν_{22}	A″	393	391	409 vw		391	391	402 vw	
ν_{23}	A′	502	502			502	502		
ν_{24}	A′	515	515	513 s	512 w	515	514	514 s	
ν_{25}	A′	583	583			583	583	589 vw	
ν_{26}	A′	597	596	613 m	612 w	597	596	612 w	
ν_{27}	A″	655	656			655	656		
ν_{28}	A″	658	658	671 vw	666 s	658	658	668 w	664 m
ν_{29}	A′	741	740			741	740		
ν_{30}	A″	741	741			741	741		
ν_{31}	A′	747	747	749 w	738 w	747	746	745 w	
ν_{32}	A′	780	779			780	779		
ν_{33}	A′	812	811		792 w	812	811	806 w	
ν_{34}	A′	835	835	815 s	811 vw	835	835	815 s	822 w
ν_{35}	A″	836	835	837 w	846 m	836	835	837 w	
ν_{36}	A′	850	848	857 w	861 m	849	848	854 w	857 w
ν_{37}	A″	883	884			883	884	872 vw	
ν_{38}	A″	890	889			889	888		
ν_{39}	A′	953	953			953	953		
ν_{40}	A′	964	963	969 vw		964	963	967 vw	
ν_{41}	A″	980	980			980	980		
ν_{42}	A′	983	981			981	980		
ν_{43}	A′	984	982	989 vw	990 vw	983	982	985 vw	
ν_{44}	A′	1000	998			998	999		
ν_{45}	A″	1002	1002			1002	1002		
ν_{46}	A′	1008	1008			1008	1008		

Table 3 continued

No	Symm. Spec	Hg (Bpp)Cl_2				Hg (Bpp)Br_2			
		LANL2DZ[a] Freq.[a]	SDD[b] Freq.[b]	Exp. IR	Exp. RA	LANL2DZ[a] Freq.[a]	SDD[b] Freq.[b]	Exp. IR	Exp. RA
ν_{47}	A″	1013	1013	1013 s	1014 vs	1014	1013	1013 s	1013 m
ν_{48}	A′	1046	1047		1031 w	1046	1046		1028 s
ν_{49}	A′	1050	1049			1050	1049		
ν_{50}	A″	1061	1060	1071 m	1071 m	1061	1061	1070 m	1067 w
ν_{51}	A″	1092	1092	1105 vw		1093	1092	1105 w	
ν_{52}	A″	1117	1116	1155 vw		1117	1117		1150 w
ν_{53}	A′	1201	1201			1201	1201		
ν_{54}	A′	1204	1204			1205	1204		
ν_{55}	A′	1207	1207	1211 s	1216 s	1207	1207	1209 s	1216 s
ν_{56}	A′	1216	1214	1219 vw		1216	1214	1221 w	1227 vw
ν_{57}	A″	1230	1230			1230	1230		
ν_{58}	A′	1243	1242			1243	1243		
ν_{59}	A″	1260	1260	1255 vw	1247 vw	1260	1260	1258 vw	
ν_{60}	A″	1273	1273			1273	1273		
ν_{61}	A″	1276	1276		1280 w	1276	1276	1275 vw	
ν_{62}	A′	1311	1310			1311	1311		
ν_{63}	A″	1327	1327	1322 vw	1326 m	1327	1327	1321 vw	1322 s
ν_{64}	A′	1333	1332	1352 w	1345 w	1333	1332	1352 w	
ν_{65}	A″	1334	1332	1375 vw		1334	1332	1375 vw	
ν_{66}	A″	1388	1387	1397 vw		1388	1387	1391 vw	
ν_{67}	A″	1406	1405	1429 s	1434 m	1405	1404	1428 s	1437 s
ν_{68}	A′	1454	1453	–		1454	1453	1446 vw	
ν_{69}	A′	1459	1458	1456 m		1459	1458	1457 m	
ν_{70}	A′	1466	1466			1466	1466		
ν_{71}	A′	1469	1468			1470	1468		
ν_{72}	A′	1479	1478	1475 vw		1479	1478	1475 vw	
ν_{73}	A″	1534	1534	1503 m	1505 m	1534	1533	1501 m	
ν_{74}	A″	1540	1539	1542 vw		1540	1539	1541 vw	
ν_{75}	A′	1569	1568	1561 m	1557 m	1569	1569	1561 m	
ν_{76}	A′	1585	1584	1611 vs	1611 s	1585	1584	1610 vs	1611 s
ν_{77}	A′	2926	2925	2926 vs	2922 s	2926	2925	2926 m	2928 vs
ν_{78}	A′	2930	2929			2930	2929		
ν_{79}	A′	2938	2937			2938	2937		
ν_{80}	A″	2966	2965	2952 s		2966	2965	2946 vs	2949 w
ν_{81}	A″	2980	2979	2983 vw	2994 vw	2980	2979	2979 vw	2996 vw
ν_{82}	A″	3004	3002			3004	3003		
ν_{83}	A″	3071	3071	3032 w	3028 vw	3071	3071	3029 w	3030 w
ν_{84}	A′	3072	3072	3057 w	3055 vs	3072	3072	3053 w	3055 vs
ν_{85}	A″	3089	3088			3088	3088		
ν_{86}	A″	3090	3090			3089	3089		
ν_{87}	A′	3092	3092			3092	3092		
ν_{88}	A′	3099	3099			3099	3099		
ν_{89}	A″	3106	3107			3106	3106		
ν_{90}	A′	3112	3112			3111	3111		
				155				110	

Table 3 continued

No	Symm. Spec	Hg (Bpp)I_2				Free Bpp [8]		TED(%)
		LANL2DZ[a]	SDD[b]	Exp. IR	Exp. RA	Exp. IR	Exp. RA	
ν_1	A″	4	2					$\Gamma_{HCCC}(65) + \Gamma_{XMNC}(22)$(M)
ν_2	A″	11	11					$\Gamma_{CCCC}(56) + \Gamma_{HCCC}(27)$(M)
ν_3	A′	14	17					$\delta_{CCC}(21)$(M) + $\Gamma_{MNCC}(17) + \Gamma_{CCCC}(15)$(M) + $\Gamma_{XMNCC}(11)$
ν_4	A″	25	29					$\Gamma_{XMNC}(75) + \Gamma_{CCCC}(14)$(M)
ν_5	A″	32	33					$\delta_{XMN}(38) + \delta_{MNC}(13) + \Gamma_{CCCC}(18)$(M) + $\Gamma_{HCCC}(15)$(M)
ν_6	A′	34	39					$\delta_{CCC}(19)$(M) + $\Gamma_{XMNC}(27) + \Gamma_{MNCC}(11)$
ν_7	A″	39	43					$\delta_{XMN}(57) + \delta_{MNC}(29)$
ν_8	A″	51	52					$\delta_{MNC}(47) + \Gamma_{HCCC}(23)$(M) + $\Gamma_{CCCC}(12)$ (M)
ν_9	A′	61	65					$\Gamma_{XMNC}(51)$(M) + $\Gamma_{CCCC}(15)$
ν_{10}	A′	91	88					$\Gamma_{HCCC}(69)$(P-M) + $\Gamma_{CCCC}(30)$(P-M) + $\Gamma_{HCCC}(13)$
ν_{11}	A′	91	90		89 s		89 s	$\upsilon_{MN}(26) + \upsilon_{MX}(33)$
ν_{12}	A″	118	122		109 vs		91 vs	$\upsilon_{MX}(24) + \Gamma_{XMNC}(12) + \Gamma_{MNCC}(11)$
ν_{13}	A′	118	127		170 vw		155 vw	$\upsilon_{MX}(11) + \delta_{MNC}(63) + \delta_{XMN}(14)$
ν_{14}	A′	130	132		213 vw		221 w	$\upsilon_{MN}(21) + \upsilon_{MX}(39)$
ν_{15}	A′	170	187		222 w			$\upsilon_{MN}(16) + \upsilon_{CC}(13)$(M) + $\delta_{CCC}(8)$(M) + $\Gamma_{CCCC}(22)$
ν_{16}	A′	224	223					$\upsilon_{MX}(19) + \delta_{CCC}(25)$(M)
ν_{17}	A″	241	241		251 s			$\upsilon_{MX}(90)$
ν_{18}	A′	327	327					$\delta_{CCC}(77)$(M)
ν_{19}	A″	333	333					$\delta_{CCC}(25)$(M) + $\Gamma_{CCCC}(18)$
ν_{20}	A″	336	336		342 w		346 w	$\delta_{CCC}(69)$(M)
ν_{21}	A″	378	378					$\Gamma_{NCCC}(41) + \Gamma_{HCCC}(34) + \Gamma_{NCCH}(14) + \Gamma_{CNCC}(12)$
ν_{22}	A″	390	390	410 vw		403 vw	410 vw	$\Gamma_{NCCC}(36)$ +$\Gamma_{CCCC}(17) + \Gamma_{CCCH}(13) + \Gamma_{NCCH}(12)$
ν_{23}	A′	501	501					$\upsilon_{C\text{-}CH2}(11) + \delta_{CCC}(11)$
ν_{24}	A′	514	514	513 s		505 s	506 w	$\Gamma_{CNCC}(11) + \Gamma_{CNCH}(10)$
ν_{25}	A′	583	583	587 vw		577 m		$\delta_{CCC}(21)$(M)
ν_{26}	A′	596	596	608 m	600 w	603 s		$\delta_{CCC}(18) + \delta_{CCC}(16) + \delta_{CNC}(10)$
ν_{27}	A″	656	656					$\delta_{NCC}(29) + \delta_{CCC}(26) + \delta_{CCH}(16)$
ν_{28}	A″	658	658	670 w	666 w	670 vw	668 m	$\delta_{NCC}(31) + \delta_{CCC}(26) + \delta_{CCH}(17)$
ν_{29}	A′	741	740					$\Gamma_{CNCC}(20) + \Gamma_{NCCC}(18)$
ν_{30}	A″	742	741					$\Gamma_{CCCH}(62)$(M)
ν_{31}	A′	747	746	741 w		743 w	745 vw	$\Gamma_{NCCC}(23) + \Gamma_{CNCC}(13)$
ν_{32}	A′	780	780					$\upsilon_{C\text{-}CH2}(26) + \upsilon_{CC}(24) + \delta_{CNC}(14)$
ν_{33}	A′	811	811	805 w				$\upsilon_{CC}(10) + \Gamma_{CCCH}(19) + \Gamma_{NCCH}(10)$
ν_{34}	A′	835	835	812 s	814 w	784 vs	799 vw	$\upsilon_{CC}(22)$(M) + $\upsilon_{CC}(15) + \Gamma_{CCCH}(23)$
ν_{35}	A″	836	836	836 w		831 s	826 w	$\delta_{CCH}(16) + \Gamma_{CCCH}(37)$(M)
ν_{36}	A′	848	848	851 w	851 m	855 s	863 m	$\Gamma_{CCCH}(35) + \Gamma_{NCCH}(15)$
ν_{37}	A″	884	884	867 vw				$\Gamma_{CCCH}(44)$(P-M) + $\Gamma_{NCCH}(22) + \Gamma_{CCCH}(17) + \Gamma_{CNCH}(16)$
ν_{38}	A″	888	888					$\Gamma_{CCCH}(34) + \Gamma_{CCCH}(22)$(P-M) + $\Gamma_{NCCH}(21) + \Gamma_{CNCH}(11)$
ν_{39}	A′	953	953					$\upsilon_{CC}(23) + \upsilon_{CN}(39) + \delta_{CCC}(14)$
ν_{40}	A′	964	963	965 vw				$\Gamma_{HCCH}(48) + \Gamma_{CCCH}(16)$
ν_{41}	A″	979	978					$\Gamma_{CNCH}(18) + \Gamma_{HCCH}(48) + \Gamma_{CCCH}(22)$
ν_{42}	A′	980	980					$\upsilon_{CC}(14) + \Gamma_{HCCH}(34) + \Gamma_{CCCH}(10)$
ν_{43}	A′	982	981	982 vw		991 s	994 s	$\upsilon_{CC}(20) + \upsilon_{CC}(12)$(M) + $\upsilon_{CN}(25)$
ν_{44}	A′	997	997					$\upsilon_{CC}(59)$(M)

Table 3 continued

No	Symm. Spec	Hg (Bpp)I_2				Free Bpp [8]		
		LANL2DZ[a]	SDD[b]	Exp. IR	Exp. RA	Exp. IR	Exp. RA	TED(%)
ν_{45}	A″	1002	1002					$\Gamma_{HCCC}(20) + \Gamma_{HCCH}(42) + \Gamma_{CNCH}(14) + \Gamma_{MNCH}(14)$
ν_{46}	A′	1008	1008					$\upsilon_{CC}(58) + \delta_{HCC}(13)(M)$
ν_{47}	A″	1014	1014	1010 s	1009 s			$\upsilon_{CC}(14) + \delta_{HCC}(19)(M) + \Gamma_{HCCC}(16)(Py\text{-}M) + \Gamma_{HCCH}(23)$
ν_{48}	A′	1046	1046	1025 vw	1025 s	1021 w	1021 w	$\upsilon_{CC}(11) + \upsilon_{CN}(27) + \delta_{CCC}(11) + \delta_{NCC}(12) + \delta_{CCH}(24)$
ν_{49}	A′	1050	1049					$\upsilon_{CC}(12) + \upsilon_{CN}(20) + \delta_{CCC}(12) + \delta_{NCC}(14) + \delta_{CCH}(27)$
ν_{50}	A″	1061	1061	1067 m	1067 m	1065 w	1077 w	$\upsilon_{CC}(15) + \delta_{CCH}(15)(M)$
ν_{51}	A″	1093	1093	1104 vw				$\upsilon_{CC}(21) + \delta_{CCH}(21)(M)$
ν_{52}	A″	1118	1117	1153 vw				$\upsilon_{CC}(10) + \delta_{CCH}(21) + \delta_{CCH}(18)(M)$
ν_{53}	A′	1202	1201					$\upsilon_{CC}(10) + \upsilon_{C\text{-}CH2}(31) + \delta_{CCH}(25)$
ν_{54}	A′	1205	1204					$\upsilon_{CC}(18) + \upsilon_{CN}(14) + \delta_{CCH}(29) + \delta_{NCH}(23)$
ν_{55}	A′	1207	1207	1210 s	1214 s	1215 m	1218 s	$\upsilon_{C\text{-}CH2}(28) + \delta_{CCH}(28)$
ν_{56}	A′	1215	1214	1221 w		1227 m		$\upsilon_{CC}(25) + \upsilon_{CN}(10) + \upsilon_{C\text{-}CH2}(10) + \delta_{CCH}(18) + \delta_{NCH}(22)$
ν_{57}	A″	1231	1230					$\delta_{CCH}(25)(M)$
ν_{58}	A′	1244	1243					$\delta_{CCH}(49)(M) + \Gamma_{HCCH}(15)(M)$
ν_{59}	A″	1260	1260	1256 vw		1252 vw	1253 w	$\upsilon_{CC}(22) + \upsilon_{CN}(37)(M)$
ν_{60}	A″	1273	1273					$\upsilon_{CN}(13) + \delta_{CCH}(43)(M)$
ν_{61}	A″	1276	1276	1273 vw				$\upsilon_{CC}(23) + \upsilon_{CN}(40) + \delta_{CCH}(23)(M)$
ν_{62}	A′	1312	1312					$\delta_{CCH}(40) + \Gamma_{HCCH}(22)(Py\text{-}M)$
ν_{63}	A″	1327	1327	1327 vw	1318 m	1318 vw	1318 vw	$\delta_{CCH}(59) + \delta_{NCH}(18)$
ν_{64}	A′	1333	1333	1350 w		1340 m	1341 m	$\delta_{CCH}(41) + \Gamma_{HCCH}(19)(M)$
ν_{65}	A″	1333	1333					$\delta_{CCH}(60) + \delta_{NCH}(16)$
ν_{66}	A″	1388	1387	1386 vw		1376 vw		$\upsilon_{CC}(23) + \delta_{CCH}(24) + \delta_{NCH}(31)$
ν_{67}	A″	1403	1403	1426 s	1435 m	1416 s	1411 m	$\upsilon_{CC}(32) + \delta_{CCH}(23) + \delta_{NCH}(30)$
ν_{68}	A′	1454	1453	1447 vw		1441 w	1440 m	$\upsilon_{CN}(12) + \delta_{CCH}(36) + \delta_{NCH}(20)$
ν_{69}	A′	1459	1458	1457 m		1456 m		$\delta_{HCH}(27) + \Gamma_{HCCH}(24) + \Gamma_{HCCC}(14)(M)$
ν_{70}	A′	1466	1466					$\delta_{HCH}(30)(M) + \Gamma_{HCCH}(22) + \Gamma_{HCCC}(13)(M)$
ν_{71}	A′	1469	1469					$\upsilon_{CC}(13) + \delta_{CCH}(48) + \delta_{NCH}(19)$
ν_{72}	A′	1479	1478	1475 vw		1475 vw		$\delta_{HCH}(30) + \Gamma_{HCCH}(29)(M)$
ν_{73}	A″	1534	1534	1501 m		1501 m	1509 vw	$\upsilon_{CC}(49) + \upsilon_{CN}(24)$
ν_{74}	A″	1540	1539	1542 vw		1542 vw		$\upsilon_{CC}\ (48) + \upsilon_{CN}(27)$
ν_{75}	A′	1569	1569	1560 m		1557 m	1557 w	$\upsilon_{CC}(50) + \delta_{CCH}(18)$
ν_{76}	A′	1584	1583	1608 vs	1610 m	1605 vs	1606 m	$\upsilon_{CC}(59)$
ν_{77}	A′	2926	2925	2924 m	2924 s	2929 w	2927 w	$\upsilon_{CH2}(100)$
ν_{78}	A′	2930	2929					$\upsilon_{CH2}(100)$
ν_{79}	A′	2938	2937					$\upsilon_{CH2}(100)$
ν_{80}	A″	2966	2965	2940 vs	2942 w	2944 vs		$\upsilon_{CH2}(100)$
ν_{81}	A″	2980	2979	2977 vw		2971	2975	$\upsilon_{CH2}(99)$
ν_{82}	A″	3004	3003					$\upsilon_{CH2}(100)$
ν_{83}	A″	3071	3071	3026 w	3026 w	3029 m	3031 w	$\upsilon_{CH}(100)$
ν_{84}	A′	3072	3072	3049 w	3050 vs	3051 w	3056 vs	$\upsilon_{CH}(100)$
ν_{85}	A″	3087	3086					$\upsilon_{CH}(99)$
ν_{86}	A″	3088	3088					$\upsilon_{CH}(99)$
ν_{87}	A′	3092	3092					$\upsilon_{CH}(100)$
ν_{88}	A′	3099	3099					$\upsilon_{CH}(99)$
ν_{89}	A″	3104	3104					$\upsilon_{CH}(99)$

Table 3 continued

No	Symm. Spec	Hg (Bpp)I_2				Free Bpp [8]		
		LANL2DZ[a]	SDD[b]	Exp. IR	Exp. RA	Exp. IR	Exp. RA	TED(%)
ν_{90}	A′	3109	3109					υ_{CH}(99)
				72			Total Shifts	

P: Pyridyl group, M. Methylene, scis, scissoring; rock, rocking; twist, twisting; wag, wagging; asymm, asymmetric; symm, symmetric; str, stretching; tors, torsion; bend, bending; def, deformation; vs, very strong; s, strong; m, medium; w, weak; vw, very weak; sym. Spec: symmetry species; Exp: Experimental; Freq: Frequencies [a] Scaling Factor: 0.9613, [b] Scaling Factor: 0.9612

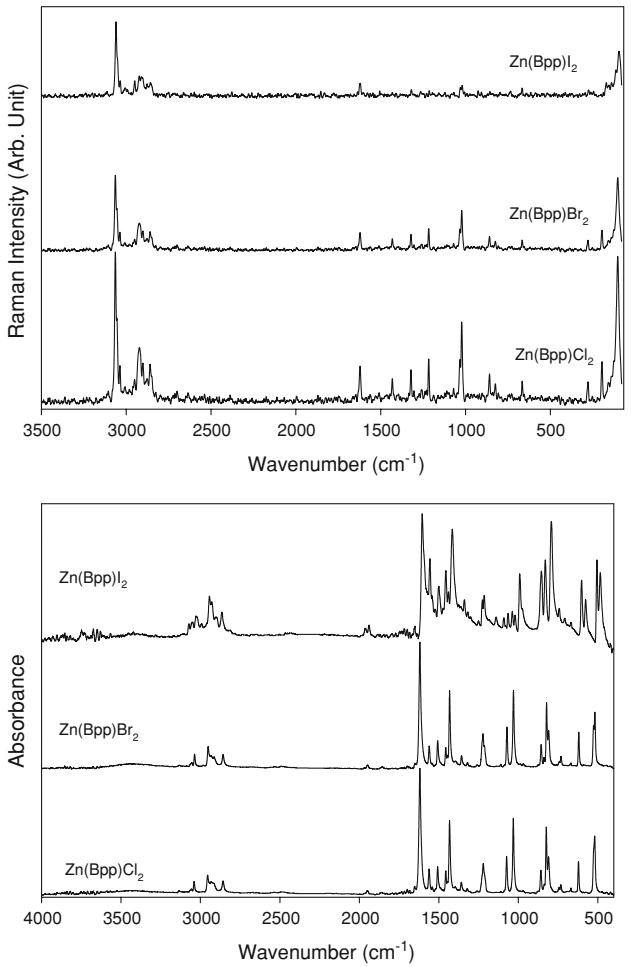

Fig. 3 The Raman and infrared spectra of $Zn(Bpp)X_2$. *X*: Cl, Br, or I

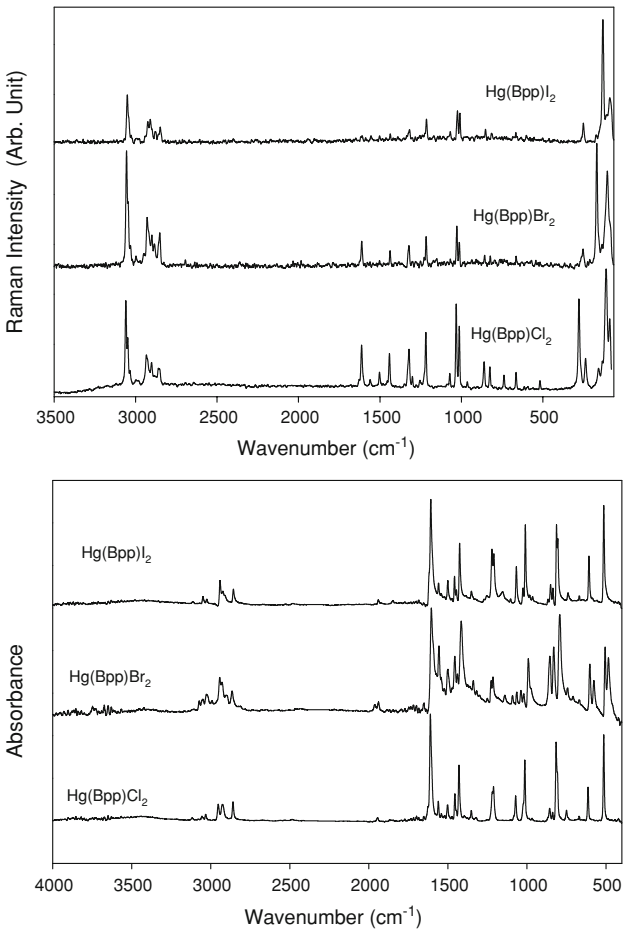

Fig. 4 The Raman and infrared spectra of $Hg(Bpp)_2X_2$. *X*: Cl, Br, and I

B3LYP functional in conjunction with the LANL2DZ and SDD basis sets approach for molecular vibrational problems. The calculated vibrational wave numbers and optimized geometric parameters were compared with experimentally derived ones. The good agreement between the frequencies calculated by density functional methods and the experimental results indicates provides solid evidence for the reliability of FT-IR and FT-Raman spectra to predict the coordination effects on Bpp vibrations. Asymmetric CH_2 stretching vibrations showed a small shift towards higher frequencies, whereas symmetric CH_2 stretching showed a small shift towards lower frequencies in the FT-IR and FT-Raman spectra of metal complexes. Ring stretching vibrations shifted to higher frequencies when free ligand was coordinated to the metal ion.

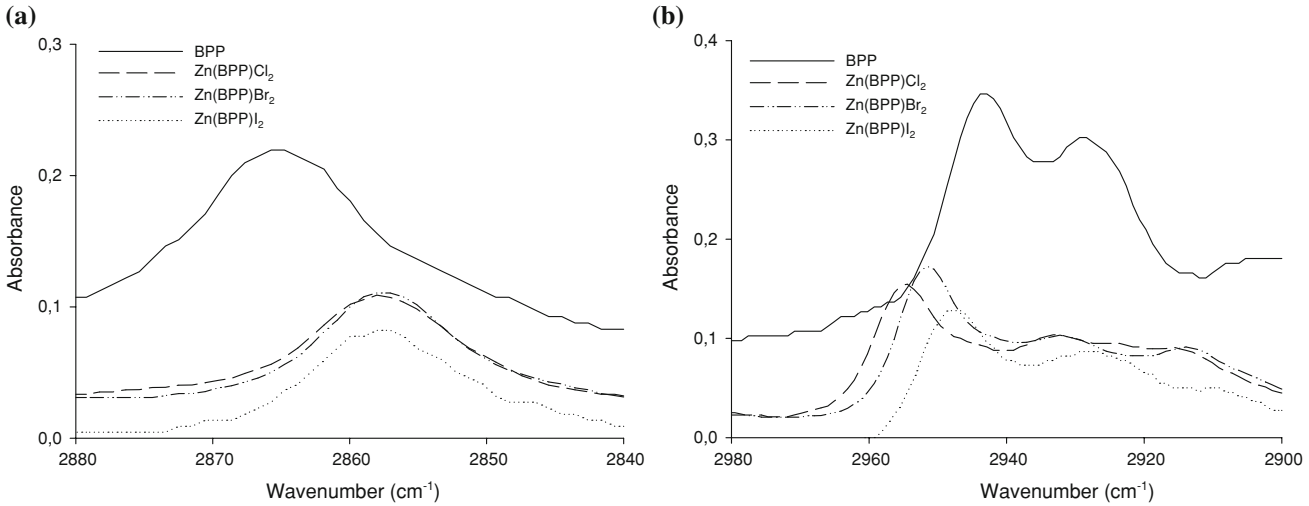

Fig. 5 The symmetric CH_2 (**a**) and the asymmetric CH_2 (**b**) stretching vibrations of Zn complexes

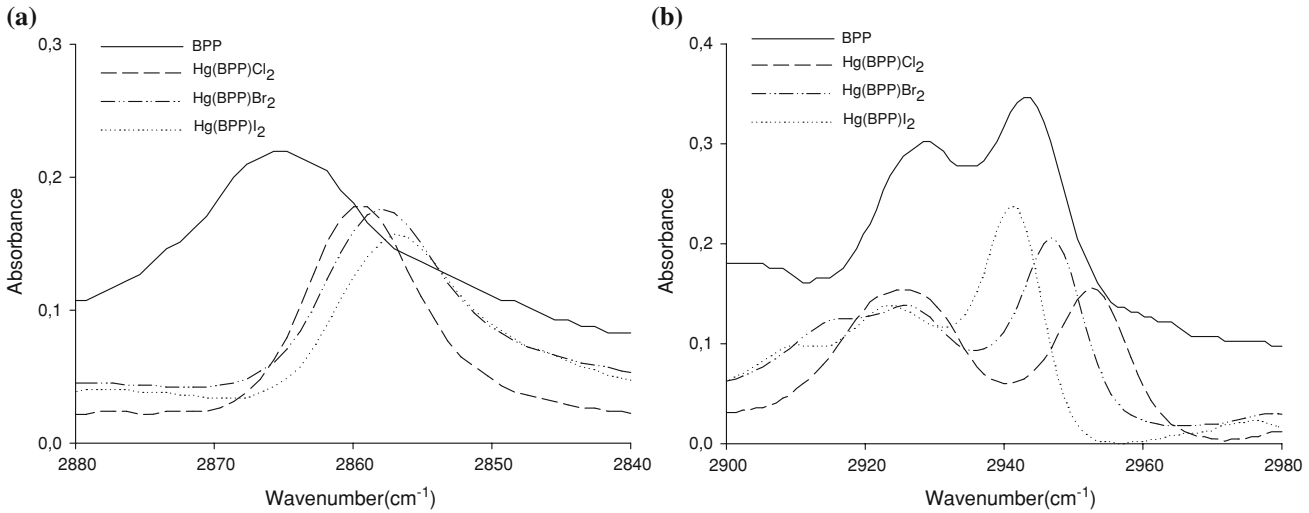

Fig. 6 The symmetric CH_2 (**a**) and the asymmetric CH_2 (**b**) stretching vibrations of Hg complexes

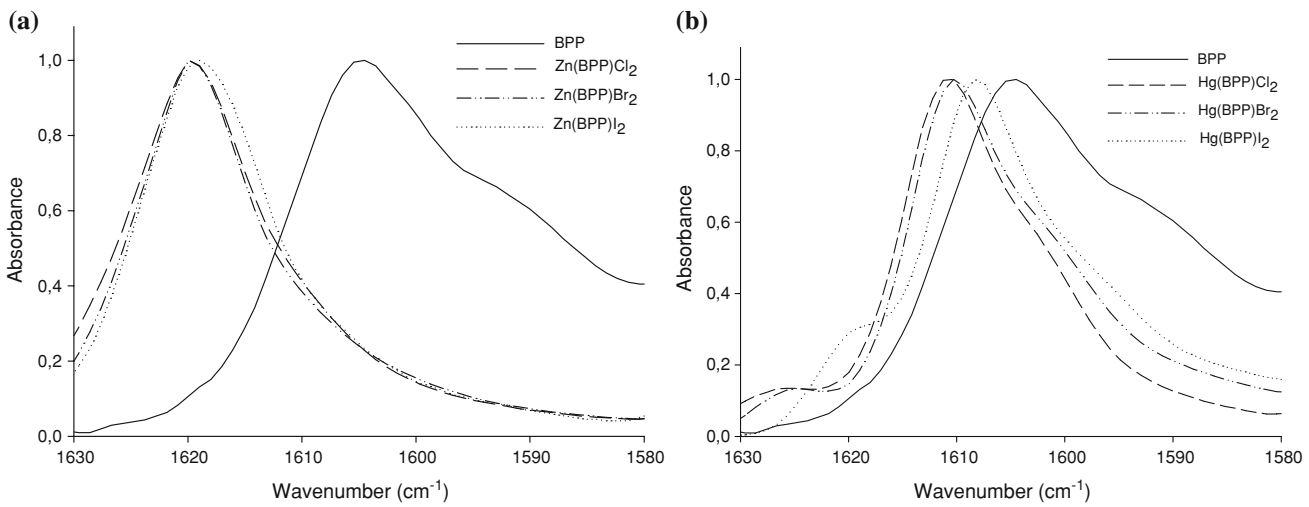

Fig. 7 The ring stretching vibrations of Zn (**a**) and Hg (**b**) complexes

Acknowledgments This work was supported by the Research Fund of the University of Gazi, project numbers: 30/2005-01. We wish to thank the central laboratory of METU for recording the Raman spectra of the samples and Gazi University, Arts and Science Faculty, Department of Chemistry, for recording the infrared spectra of the samples.

References

1. Lee, T.W., Lau, J.P.K., Wong, W.T.: Synthesis and characterization of coordination polymers of Zn(II) with 1,3-bis(4-pyridyl)propane and 4,4′-pyridine ligands. Polyhedron **23**, 999–1002 (2004). doi:10.1016/j.poly.2003.12.020
2. Correa, C.C., Diniz, R., Chagas, L.H., Rodrigues, B.L., Yoshida, M.I., Teles, W.M., Machado, F.C., Oliveira, L.F.C.: Transition metal complexes with squarate anion and the pyridyl-donor ligand 1,3-bis(4-pyridyl)propane (BPP): synthesis, crystal structure and spectroscopic investigation. Polyhedron **26**, 989–995 (2007). doi:10.1016/j.poly.2006.09.037
3. Correa, C.C., Diniz, R., Chagas, L.H., Rodrigues, B.L., Yoshida, M.I., Teles, W.M., Machado, F.C., Oliveira, L.F.C.: Synthesis, vibrational spectroscopy and crystal structures of polymers involving transition metals with squarate ions and 1,3-bis(4-pyridyl)propane. Vib. Spectrosc. **45**, 82 (2007). doi:10.1016/j.vibspec.2007.04.004
4. Plater, M.J., Foreman, M.R.S.J., Gelbrich, T., Coles, S.J., Hursthouse, M.B.: Synthesis and characterisation of infinite coordination networks from flexible dipyridyl ligands and cadmium salts. J. Chem. Soc. Dalton Trans. **18**, 3065–3073 (2000)
5. Yang, G., Jin, C., Hong, J., Guo, Z., Zhu, L.: Ab initio and density functional theory studies on vibrational spectra of palladium (II) and platinum (II) complexes of methionine and histidine: effect of theoretical methods and basis sets. Spectrochim. Acta A: Mol. Biomol. Spectrosc. **60**, 3187–3195 (2004)
6. Ceulemans, A., Chibotaru, L.F., Heylen, G.A., Pierloot, K., Vanquickenbrone, L.G.: Theoretical models of exchange interactions in dimeric transition-metal complexes. Chem. Rev. **100**, 787 (2000)
7. Keuleers, R., Desseyn, H.O., Rousseau, B., Van Alsenoy, C.: Solids modeled by ab Initio Crystal Field Methods. 21. Study of the structure and vibrational spectrum of N,N‘-Dimethylurea in the gas phase and in Its Cc crystal phase. J. Phys. Chem. A **104**(25), 5946–5954 (2000)
8. Erdoğdu, Y., Güllüoğlu, M.T., Kurt, M.: Molecular structure and vibrational spectra of 1,3-bis(4-pyridyl)propane by quantum chemical calculations. Spectrochim. Acta [A] **71**, 377–387 (2008). doi:10.1016/j.saa.2008.01.012
9. Suen, M.C., Tsai, H.A., Wang, J.C.: Synthesis and structures of infinite coordination polymers from 1,3-bis (4-pyridyl) propane ligand and zinc salts. J. Chin. Chem. Soc. **53**, 305–312 (2006)
10. Chen, Y.B., Zhang, J.K., Cheng, J.K., Kang, Y., Li, Z.J., Yao, Y.G.: 1D chain structure, NLO and luminescence properties of $^{1}_{\infty}[Zn_2(bpp)(pht)_2]$. Inorg. Chem. Commun. **7**, 1139–1141 (2004). doi:10.1016/j.inoche.2004.08.018
11. Gao, E.Q., Bai, S.Q., Wang, Z.M., Yan, C.H.: One-and two-dimensional metal-dicyanamido complexes with a flexible bridging co-ligand: structural and magnetic properties. J. Chem. Soc. Dalton Trans. **9**, 1759–1764 (2003)
12. Frisch, M.J., Trucks, G.W., Schlegel, H.B., Scuseria, G.E., Robb, M.A., Cheeseman, J.R., Montgomery Jr., J.A., Vreven, T., Kudin, K.N., Burant, J.C., Millam, J.M., Iyengar, S.S., Tomasi, J., Barone, V., Mennucci, B., Cossi, M., Scalmani, G., Rega, N., Petersson, G.A., Nakatsuji, H., Hada, M., Ehara, M., Toyota, K., Fukuda, R., Hasegawa, J., Ishida, M., Nakajima, T., Honda, Y., Kitao, O., Nakai, H., Klene, M., Li, X., Knox, J.E., Hratchian, H.P., Cross, J.B., Adamo, C., Jaramillo, J., Gomperts, R., Stratmann, R.E., Yazyev, O., Austin, A.J., Cammi, R., Pomelli, C., Ochterski, J.W., Ayala, P.Y., Morokuma, K., Voth, G.A., Salvador, P., Dannenberg, J.J., Zakrzewski, V.G., Dapprich, S., Daniels, A.D., Strain, M.C., Farkas, O., Malick, D.K., Rabuck, A.D., Raghavachari, K., Foresman, J.B., Ortiz, J.V., Cui, Q., Baboul, A.G., Clifford, S., Cioslowski, J., Stefanov, B.B., Liu, G., Liashenko, A., Piskorz, P., Komaromi, I., Martin, R.L., Fox, D.J., Keith, T., Al-Laham, M.A., Peng, C.Y., Nanayakkara, A., Challacombe, M., Gill, P.M.W., Johnson, B., Chen, W., Wong, M.W., Gonzalez, C., Pople, J.A.: Gaussian 03, Revision C.02. Gaussian, Inc., Wallingford (2004)
13. Firsch, A., Nielsen, A.B., Holder, A.L.: Gaussview Users Manual. Gaussian Inc., Pittsburgh (2001)
14. Pulay, P., Baker, J., Wolinski, K.: 2013 Green Acres Road, Suite A, Fayetteville, Arkansas, 72703, USA
15. Hong, S.J., Kwak, H., Lee, Y.M., Kim, C., Kim, Y., Kim, S.J.: Analytical sciences. X-Ray Struc. Anal. Online **21**, 203 (2005). doi:10.2116/analscix.21.x203
16. Kim, Y., Kim, S.J., Choi, S.H., Han, J.H., Nam, S.H., Lee, J.H., Kim, H.J., Kim, C., Kim, D.W., Jang, H.G.: Crystal structures and catalytic activities of Zn(II) compounds containing 1,3-bis(4-pyridyl)propane. Inorg. Chim. Acta **359**, 2534–2542 (2006). doi:10.1016/j.ica.2006.02.044
17. Niu, Y., Hou, H., Zhu, Y.: Self-assembly of d^{10} metal adduct polymers bridged by bipyridyl-based ligands. J. Cluster Sci. **14**, 483–493 (2003). doi:10.1023/B:JOCL.0000010919.75362.ac
18. Ozel, A.E., Kecek, S., Akyüz, S.: Vibrational analysis and quantum chemical calculations of 2,2′-bipyridine Zinc(II) halide complexes. J. Mol. Struct. **834**, 548–554 (2007). doi:10.1016/j.molstruc.2006.12.045
19. Akyüz, S., Dempster, A.B., Davies, J.E.D.: Solid-state vibrational spectroscopy. Part V. An infrared and Raman spectroscopic study of metal(II) halide pyridine complexes, J. Chem. Soc. Dalton Trans., 1746–1749 (1976)
20. Akyüz, S., Davies, J.E.D., Holmes, K.T.: Solid-state vibrational spectroscopy Part VI1. An infrared and raman spectroscopic study of transition metal(II)4-methylpyridine complexes. J. Mol. Struct. **42**, 59–69 (1977). doi:10.1016/0022-2860(77)87028-2
21. Yurdakul, Ş., Akyüz, S., Davies, J.E.D.: Fourier transform infrared and Raman spectra of metal halide complexes of 3,5-lutidine in relation to their structures. Spectrosc. Lett. **29**(1), 175–183 (1996). doi:10.1080/00387019608001593
22. Suzuki, S., Orville-Thomas, W.J.: Molecular force field of pyridine and its application to pyridine-metal complexes. J. Mol. Struct. **37**, 321–327 (1977). doi:10.1016/0022-2860(77)80096-3